



Investigation of Load and Pressure Distribution on Wing with Wake Rollup for Low Speed Aircraft

Laith W. Ismail

Department of Materials Engineering/ University of Technology

(Received 8 April 2008; accepted 22 July 2008)

Abstract

The presented work shows a preliminary analytic method for estimation of load and pressure distributions on low speed wings with flow separation and wake rollup phenomena's. A higher order vortex panel method is coupled with the numerical lifting line theory by means of iterative procedure including models of separation and wake rollup. The computer programs are written in FORTRAN which are stable and efficient.

The capability of the present method is investigated through a number of test cases with different types of wing sections (NACA 0012 and GA(W)-1) for different aspect ratios and angles of attack, the results include the lift and drag curves, lift and pressure distributions along the wing span taking into the consideration the effect of the angles of attack and the aspect ratios on the wake rollup. The pressure distribution on the wings shows that there is a region of constant pressure on the upper surface of the wings near the trailing edge in the middle of the wing, also there is a region of flow separation on the upper surface of the wings. A good agreement is found between the presented work results and other from previous researches.

These results show that the presented method is able to capture much of flow over wings feature like separation and wake rollup.

Introduction

In order to predict the aerodynamic forces of wings up to and beyond stall, including flow separation and wake rollup must be taken into account.

Prandtl L. and Tietjens O. G [1] Defined separation of flow first in 1904; fluid particles near the solid surface are retarded by the friction force and by the adverse pressure gradient in the free stream. If the momentum is insufficient, the particles will be brought to rest at the separation point. Downstream of the point, the adverse pressure forces will cause reverse flow. The original boundary layer either passes over the region of recirculation fluid and re-attaches to the surface or forms a wake.

In the case of finite wings, the wake is a form of vortex sheet leaves the wing. As a consequence of the pressure difference between lower and upper sides of the wing, a certain flow is caused around the lateral edges. Thus starting a pair of strong trailing vortices. The vortex sheet immediately begins to roll itself up into these

vortices; and if eventually passes all of its vortices into a pair [2].

Several methods have been developed for wing problems taking into account the interaction between the several regions of flow around the wing. The present work is a combination of a higher order vortex panel method coupled with the numerical lifting line theory by means of iterative procedure including a model of separation and a model of wake rollup.

Many studies, both theoretical and experimental have been done, affected the development of the present method. Jacob K. [3] used two-dimensional procedure combined with a lifting surface theory for the computation of the flow around wings with rear separation. The separation point was predicted by a boundary layer calculation for the attached part of flow. Good predictions for the lift were obtained and it was shown that the wake flow behavior strongly influences the drag. Cebeci T., Lark R.W., Chang K.C., Halsey N.D. and Lee K. [4] developed an interactive viscous-inviscid procedure for the

computation of viscous flow over three-dimensional wing with separation. Pressure distributions over a number of spanwise stations, and the lift curve of the complete wing were computed. Nilay [5] applied a new hybrid CFD/Discrete Vortex (CFD/VD) method in order to preserve vortices over long distances. This method couples Lifting-Line/Free-Wake method and research in the tip vortex and the wake of a fixed wing, the indication that the tip vortex shed from the wing tip is preserved over long distance when the hybrid CFD/DV method is applied, as a starting point before attempting to simulate rigid rotor flow field.

Theory

1. Potential Flow

A higher order vortex panel method is developed from the source-vortex panel method [6] and reformulated in a manner suitable for the present model. For potential flow, the Navier-Stokes equations are reduced to the Euler's equation of motion:

$$\frac{\partial \bar{V}}{\partial t} + (\bar{V} \cdot \nabla) \bar{V} = -\frac{1}{\rho} \nabla P \quad \dots (1)$$

where $\nabla \cdot \bar{V} = 0$ (equation of continuity).

The total potential of the flow field may be written as:

$$\phi = \phi_\infty + \phi_V \quad \dots (2)$$

Where ϕ_∞ is the potential due to the uniform onset flow, and ϕ_V the perturbation velocity potential due to the boundary surfaces.

From eq. (2), the potential at arbitrary point (P) is:

$$\phi_P = V_\infty (x_P \cos \alpha + y_P \sin \alpha) - \sum_{j=1}^N \int_{panel_j} \frac{\gamma(s_j)}{2\pi} \theta_P ds_j \quad \dots (3)$$

The vorticity at any point along the panel is given by:

$$\gamma(s_j) = \gamma_j + \frac{s_j}{L_j} (\gamma_{j-1} - \gamma_j) \quad \dots (4)$$

The velocity components u and v in x and y directions respectively at the control point of the i^{th} panel due to the vortex distribution on the j^{th} panel are calculated from [7]:

$$u(x_{Pi}, y_{Pi}) = u_{Pi} = \frac{\partial \phi_P}{\partial x} = V_\infty \cos \alpha + \sum_{j=1}^N u_{V_j} \quad \dots (5)$$

$$v(x_{Pi}, y_{Pi}) = v_{Pi} = \frac{\partial \phi_P}{\partial y} = V_\infty \sin \alpha + \sum_{j=1}^N v_{V_j}$$

The surface velocity may be directly obtained from:

$$V_i = |\gamma_i| \quad \text{for } i = 1, \dots, N$$

The pressure is calculated from the velocities according to Bernoulli equation as shown below:

$$C_{P_i} = 1 - \left(\frac{V_i}{V_\infty} \right)^2 \quad \text{for } i = 1, \dots, N \quad \dots (6)$$

$$\text{where } C_p = \frac{P - P_\infty}{q_\infty}$$

2. Boundary Layer

The laminar separation criterion by Curle and Skan [8] is used, when the pressure gradient parameter is:

$$\lambda = \frac{\delta_2^2}{\nu} \frac{dV_e}{ds} \leq -0.09 \quad \dots (7)$$

The location of natural transition is obtained using Michel's method [9] when:

$$Re_{\delta_{2tr}} = 1.174 \left[1 + \frac{22400}{Re_s} \right] Re_s^{0.46} \quad \dots (8)$$

3. Wake Shape Iteration

The iteration loop for wake shape is the inner loop and involves the potential flow analysis; within this loop the separation point is fixed. A local free vortex sheet panel correction angle is computed from the following equations:

$$\Delta \theta_i = \sin^{-1} \left(\frac{\bar{V}_i \cdot \bar{n}_i}{|\gamma_{sep}|} \right) \quad \text{for upper free vortex sheet} \quad \dots (9)$$

$$\Delta \theta_i = \sin^{-1} \left(\frac{\bar{V}_i \cdot \bar{n}_i}{|\gamma_i|} \right) \quad \text{for lower free vortex sheet}$$

4. Rolling Up of the Trailing Vortex Sheet

The wake behind lifting wings tends to follow the local velocity so that the wake will carry no loads.

The vortices shed into the wake flow will eventually rollup near the wing tips to form single vortex patterns and tip vortices [5]. The trailing vortex sheet strength is equal to:

$$\gamma(z) = \frac{d\Gamma}{dz} \quad \dots (10)$$

The circulation or the strength of the i^{th} vortex located at (z_i, y_i) is:

$$g_i = \int_{z-\frac{b}{2m}}^{z+\frac{b}{2m}} \gamma dz = \int_{z-\frac{b}{2m}}^{z+\frac{b}{2m}} \frac{d\Gamma}{dz} dz \quad \dots (11)$$

Where z_i is the initial abscissa of the point vortex and $y_i = 0$ at the same time. The lift and induced drag coefficients are obtained from:

$$C_L = \frac{2}{V_\infty a} \int_{-b/2}^{b/2} \Gamma(z) dz \quad \dots(12)$$

$$C_D = \frac{2}{V_\infty a} \int_{-b/2}^{b/2} \Gamma(z) \sin \alpha_i dz$$

The induced velocity W_i of the i^{th} vortex, induced by the j^{th} vortex at (z_j, y_j) is:

$$W_i = \frac{g_j}{2\pi R} \quad \dots(13)$$

where $R = \sqrt{(z_i + z_j)^2 + (y_i + y_j)^2}$

The components of W_i are:

$$u_i = W_i \sin \theta = \frac{y_i - y_j}{R} W_i \quad \dots(14)$$

$$u_i = -W_i \cos \theta = \frac{z_i - z_j}{R} W_i$$

Adding the contributions from all vortices other than the i^{th} vortex itself and replacing u by $\frac{dz}{dt}$ and v by $\frac{dy}{dt}$ then:

$$\frac{dz_i}{dt} = \sum_{j \neq i}^m \frac{g_j}{2\pi} \frac{y_i - y_j}{(z_i - z_j)^2 + (y_i - y_j)^2} \quad \dots(15)$$

$$\frac{dy_i}{dt} = \sum_{j \neq i}^m \frac{g_j}{2\pi} \frac{z_i - z_j}{(z_i - z_j)^2 + (y_i - y_j)^2}$$

Eq. (15) form a system of two simultaneous 1st order ordinary differential equation:

$$\frac{dz}{dt} = F_1(z, y) \quad \dots(16)$$

$$\frac{dy}{dt} = F_2(z, y)$$

The solution can be obtained using the 4th order Rung-Kutta method [10] and the location of each discrete vortex in the vortex sheet can be calculated. The new location of all vortices will represent the shape of the trailing vortex sheet behind the wing.

Results and Discussion

The capability of the present method for the estimation of load and pressure distributions on rectangular wings with wake rollup will be investigated in a number of test cases. These cases, with different types of wing sections (NACA 0012 and GA(W)-1).

Fig. (1) illustrate the effect of aspect ratio on the lift curve, (a) for wing section NACA 0012, (b) for wing section GA(W)-1. It is found that the increase of lift curve slop with increasing aspect ratio. The stall for NACA 0012 occurs at about ($\alpha = 18\text{deg.}$) for (AR=5), while for GA(W)-1 beginning at ($\alpha = 20\text{deg.}$) for (AR=5). Fig. (2) illustrate the effect of aspect ratio on the drag polar, it is shown that the drag coefficient increases rapidly as the lift coefficient increased and the drag coefficient is inversely proportional to aspect ratio. A good agreement was found between the presented work data and others from [11] shown in Fig. (3).

Figs. (4) and (5) shows the local lift coefficient C_l with reference to the total lift coefficient C_L along the span. When the aspect ratio increases the lift distribution approaches more and more like rectangular distribution, for small aspect ratio the lift distribution is elliptic.

Figs. (6) and (7) shows three-dimensional pressure distribution on the upper surface of the span for different aspect ratios. For all cases, the buildup in pressure near the leading edge towards the middle of the wing is shown. The suction on the upper surface is increase with increasing aspect ratio. Also, there is a region of constant pressure on the upper surfaces of the wings near the trailing edge in the middle of the wings. This indicates that there is a flow separation at these regions and this phenomenon is expected at high angles of attack.

Fig. (8) illustrate the rolled-up wake sheet for rectangular wing with NACA 0012 airfoil compared at the same conditions from [12]. It is found that the spiral motion is observed on the wake element over the tip region during the rollup process, while the wake sheet remains relatively flat at the middle of the wing. A good agreement was found between the presented work results and others from [12].

Fig. (9) illustrate a comparison between the present method results for rectangular wing with NACA 0012 and others for [13] for the effects of angle of attack and aspect ratio shown in (a) and (b) on the rolled-up wake geometry. It is shown that the wake deformation is more pronounced at higher angle of attack and aspect ratio. A good agreement was found at this comparison.

Conclusions

1. The lift coefficient is predicted well by present method. The lift curve slope, the smooth variation with angle of attack is all good predicted.
2. The drag coefficient increases rapidly as the lift coefficient increased and the drag coefficient is inversely proportional to aspect ratio.
3. At low aspect ratio the stall occurs at higher angles of attack. Separation begins at the station of maximum local lift in the middle of the wings.
4. Finally, the developed method can be used successfully as a preliminary analysis tool for estimation of load and pressure distributions on low speed wings with wake rollup.

Nomenclature

AR	Aspect ratio	-
a	Wing area	m^2
C_D	Wing drag coefficient	-
C_L	Wing lift coefficient	-
C_l	Airfoil lift coefficient	-
C_p	Pressure coefficient	-
g_i	Strength of i^{th} vortex	$m^3/s.m$
L	Length of a panel	m
N	Number of surface panels	-
\bar{n}	Unit normal vector	-
P	Pressure	N/m^2
q	Dynamic pressure	N/m^2
Re_s	Reynolds number at surface distance	-

$Re_{\delta_{2tr}}$	Reynolds number at momentum thickness	-
s	Surface distance (distance along the panel)	m
t	Time	$sec.$
u	Velocity component in x-direction	m/s
V	Velocity	m/s
V_e	Velocity at the edge of the boundary layer	m/s
\bar{V}	Total velocity vector	m/s
v	Velocity component in y-direction	m/s
x	Chordwise coordinate	m
y	Normal coordinate	m
z	Spanwise coordinate	m
α	Angle of attack	$deg.$
α_g	Geometric angle of attack	$deg.$
Γ	Circulation	m^2/s
γ	Vorticity strength	$m^3/s.m$
γ_{sep}	Vorticity strength at separation point	$m^3/s.m$
δ_2	Momentum thickness	m
θ	Inclination of panel with x-direction	$deg.$
λ	Pressure gradient parameter	-
ρ	Density	kg/m^3
ϕ	Velocity potential	m^2/s

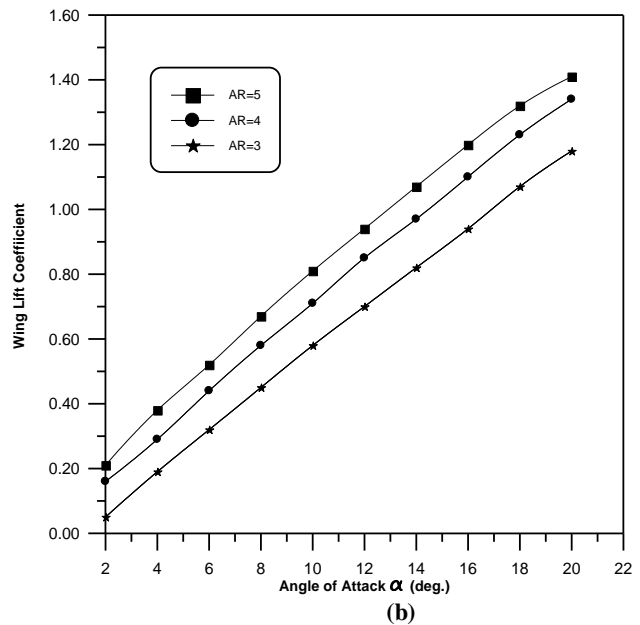
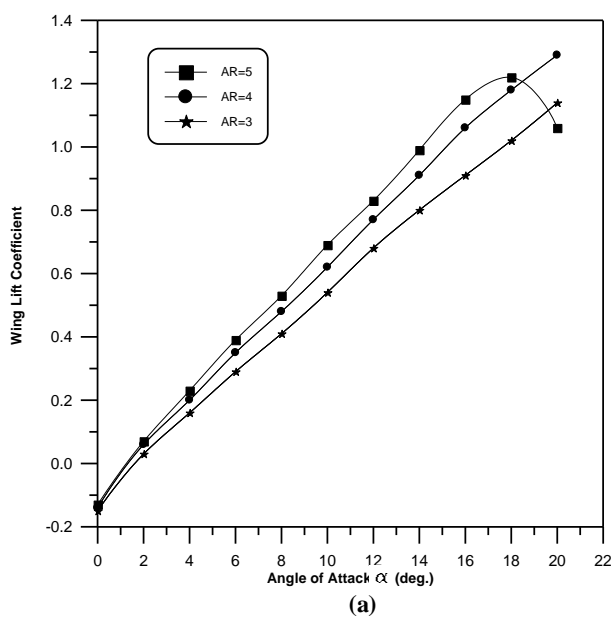


Fig. 1. Aspect Ratio Effect on the Lift Coefficient Wing Section NACA 0012 (a) Wing Section GA(W)-1 (b)

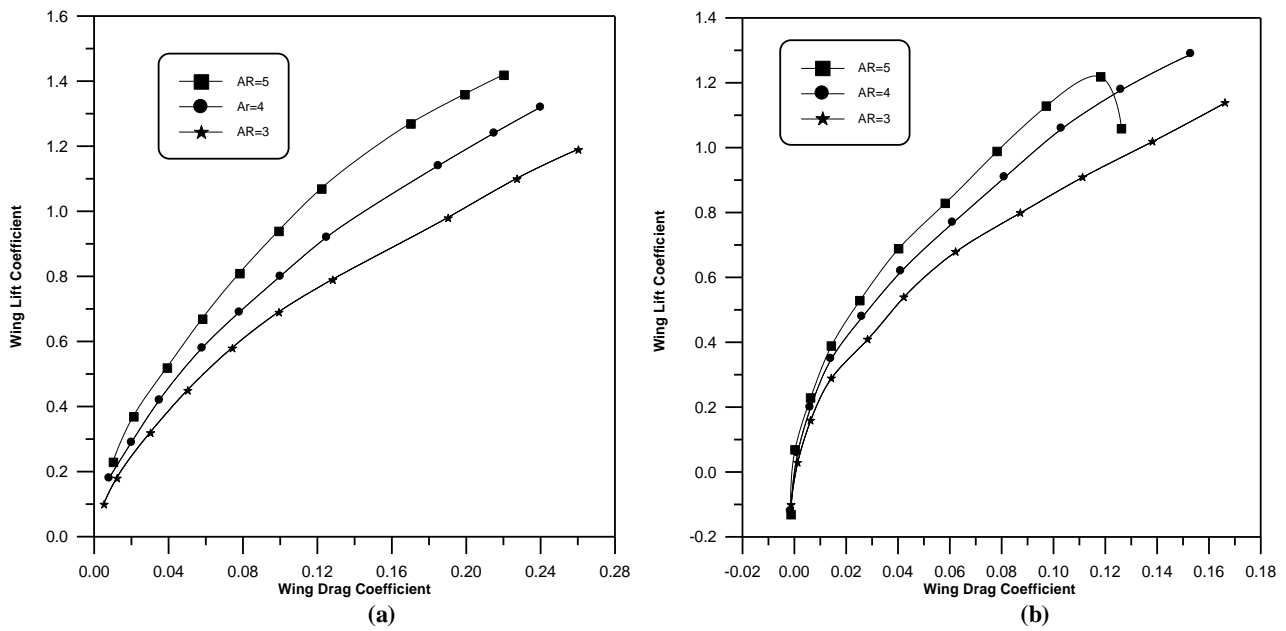


Fig. 2. Aspect Ratio Effect on the Drag Polar (a) Wing Section NACA 0012 (b) Wing Section GA(W)-1

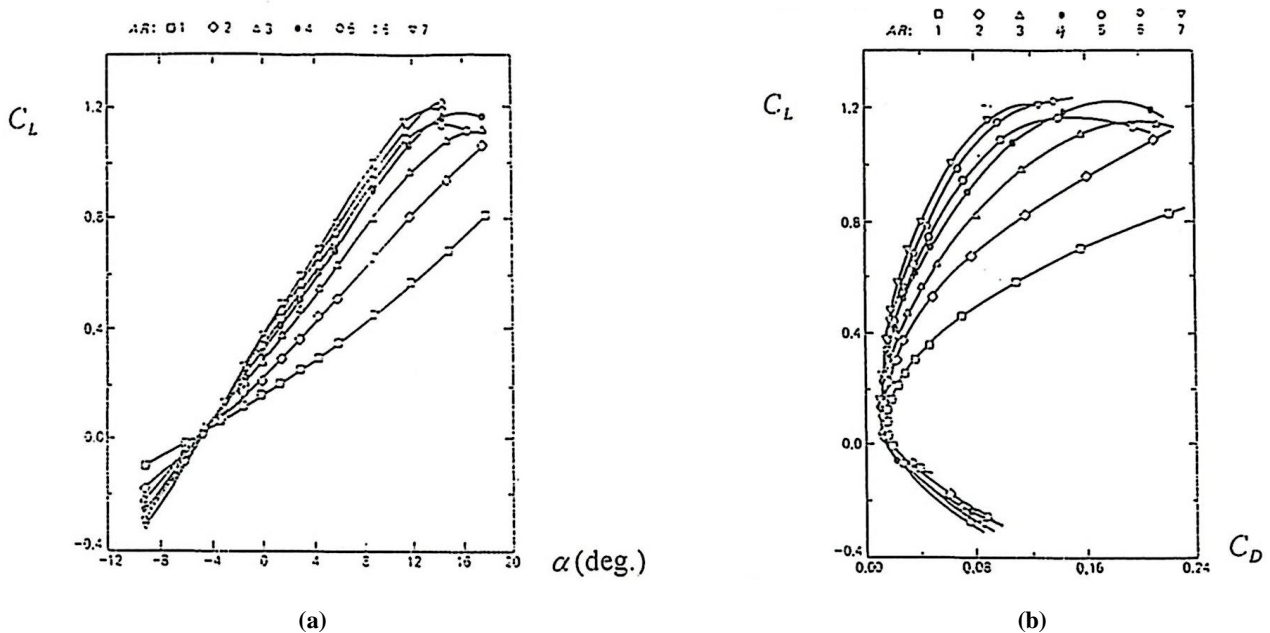


Fig. 3. (a) Aspect Ratio Effect on Lift coefficient for Rectangular Wing (b) Aspect Ratio Effect on Drag Polar for Rectangular Wing [11]

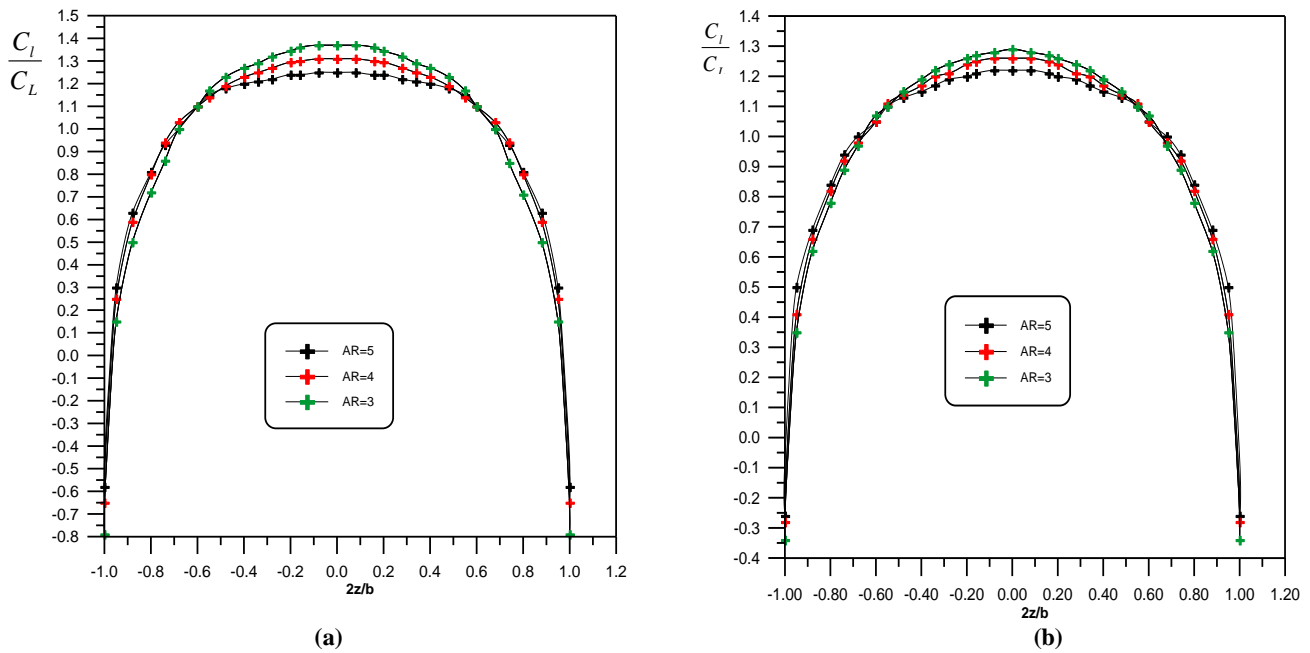


Fig. 4. Spanwise Lift Distribution on a Rectangular Wing Section NACA 0012 (a) $\alpha_g = 6$ deg. (b) $\alpha_g = 12$ deg.

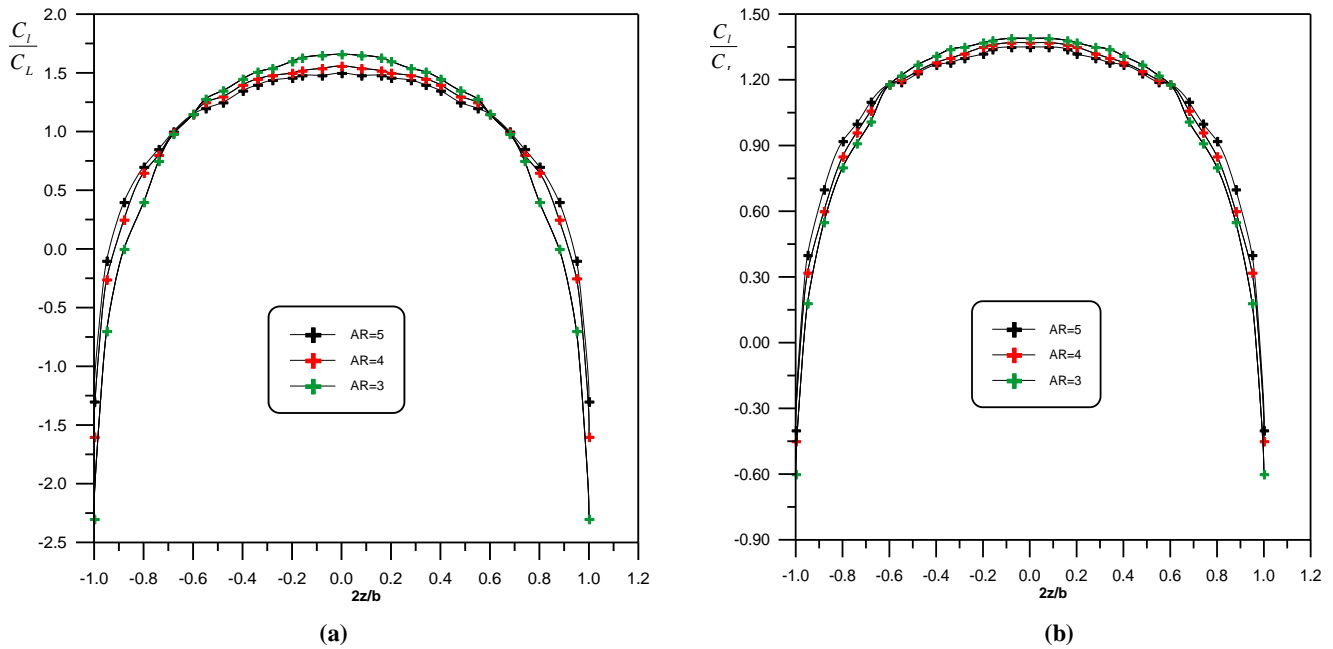


Fig. 5. Spanwise Lift Distribution on a Rectangular Wing Section GA(W)-1 (a) $\alpha_g = 6$ deg. (b) $\alpha_g = 12$ deg.

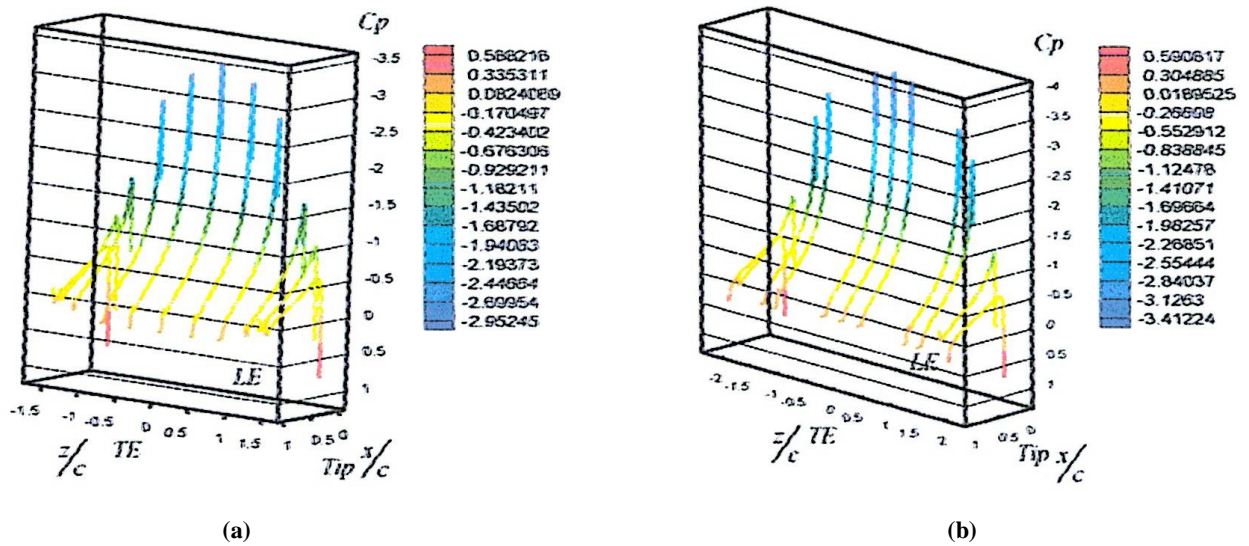


Fig. 6. Pressure Distribution on the Upper Surface of Wing with NACA 0012 (a) AR=3 (b) AR=4.

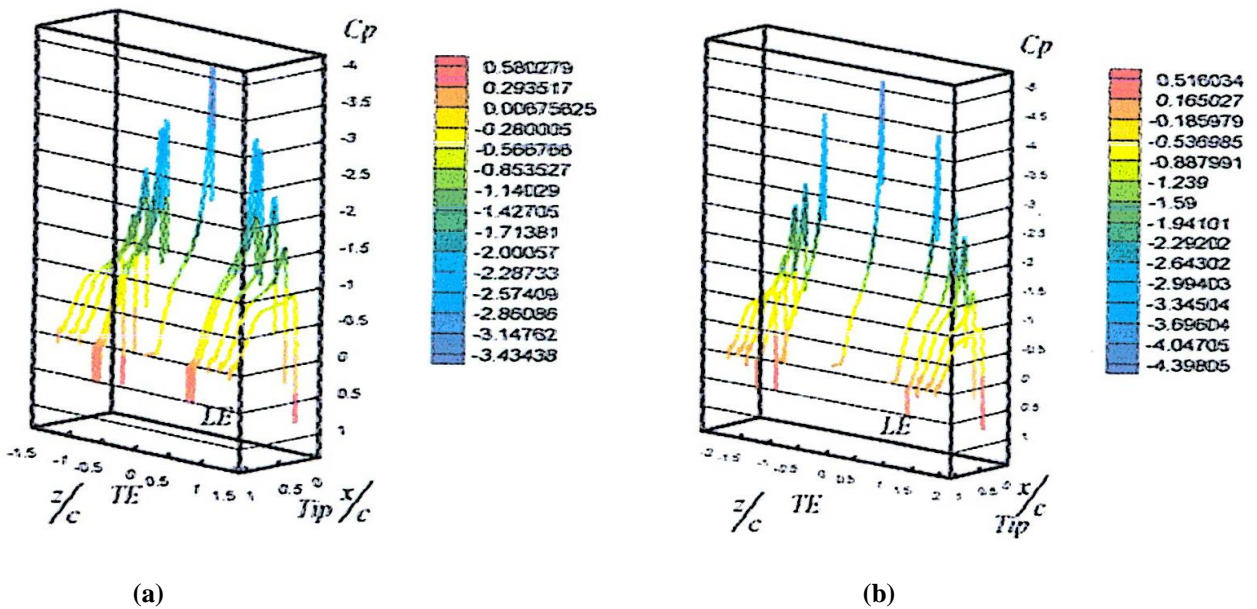


Fig. 7. Pressure Distribution on the Upper Surface of Wing with GA(W)-1 (a) AR=3 (b) AR=4.

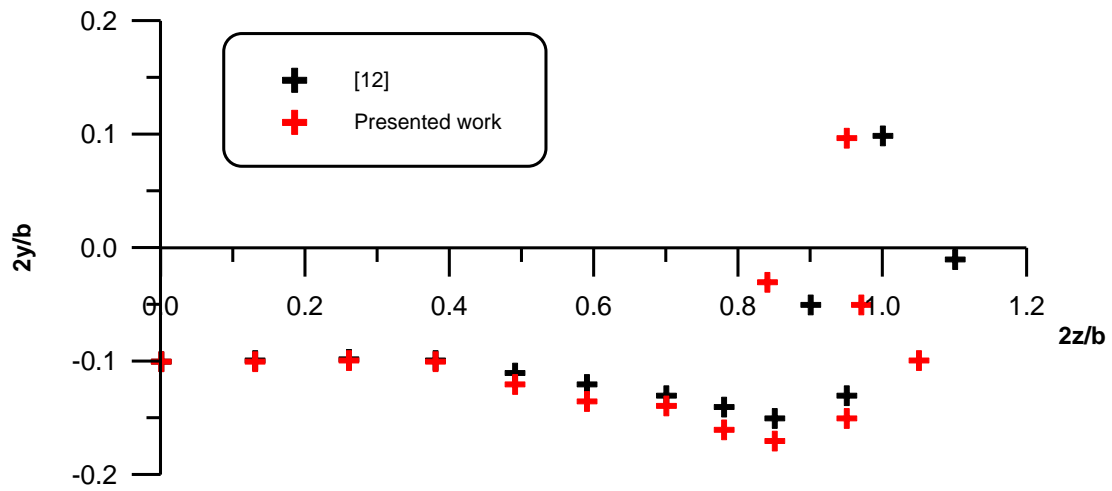


Fig. 8. Rolling Up Tip Vortices of a Rectangular Wing with NACA 0012 for AR=8 and $\alpha = 5$ deg .

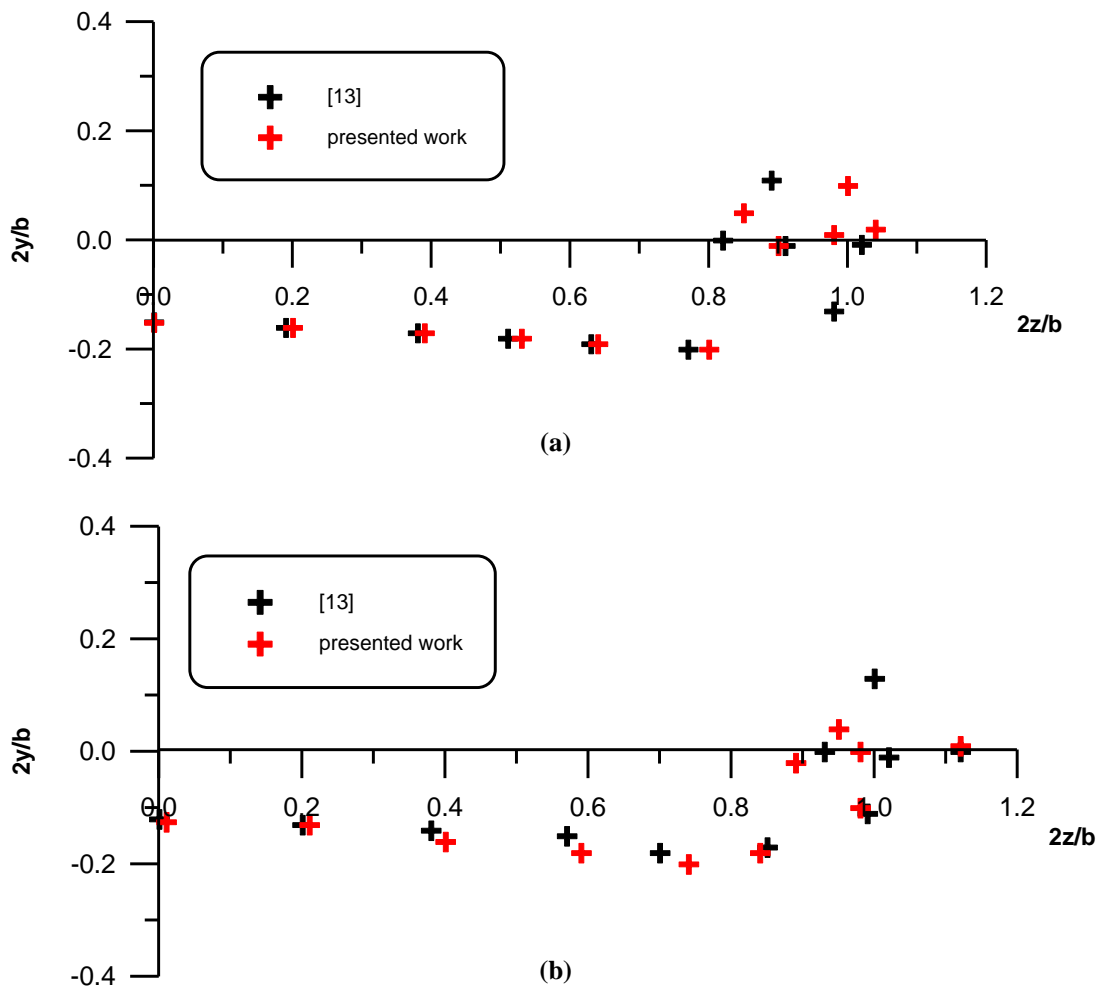


Fig. 9. Angle of Attack and Aspect Ratio Effect on the Wake Section for Rectangular Wing NACA 0012 (a) AR=8 and $\alpha = 10$ deg. (b) AR=6 and $\alpha = 6$ deg .

References

- [1] Prandtl L. and Tietjens O. G. "Fundamentals of Hydro- and Aerodynamics", Dover 216.
- [2] Sighard F. Hoerner "Fluid – Dynamic Lift", Practical Information on Aerodynamic and Hydrodynamic Lift, 1985.
- [3] Jacob K. "Computation of the Flow around Wings with Rear Separation", Journal of Aircraft, Vol.21, No. 2, February 1984, PP.97-98.
- [4] Cebeci T., Lark R.W., Chang K.C., Halsey N.D. and Lee K. "Airfoils with separation and the resulting Wake", Journal of Fluid Mechanics, Vol. 163, February 1986, PP. 323-347.
- [5] Nilay Sezer-Uzol "High – Accuracy Wake and vortex Simulations Using a Hybrid Euler/ Discrete Voortex Method", M.Sc. Thesis, Department of Aerospace Engineering, the Pennsylvania State University, May 2001.
- [6] Moran J., Cole K. and Wahl D. "Analysis of Two-Dimensional Incompressible flows by a Subsurface Panel method", AIAA Journal, Vol. 18, No. 5, May 1980, PP.526-533.
- [7] Moran J. "An Introduction to Theoretical and Computational Aerodynamics", John Wiley & Sons, 1984.
- [8] Chang P. K. "Control of Flow Separation", McGraw-Hill Book Company, 1976.
- [9] Leishman J. G., Galbraith R. A. and Hanna J. "Modeling of Trailing Edge Separation on Arbitrary Two-Dimensional Aerofoils in Incompressible Flow Using an Inviscid Flow Algorithm", Glasgow University Aero Report No. 8202, May 1982.
- [10] Chow C. Y. "An Introduction to Computational Fluid Mechanics", John Wiley & Sons. 1979.
- [11] John J. Bertin and Michael L. Smith "Aerodynamic for Engineers", Prentice-Hall, 1979.
- [12] Yeh and A. Plotkin "Vortex Panel Calculation of Wake Rollup Behind a Large Aspect Ratio Wing", AIAA Journal, Vol. 24, No. 9, September 1986, PP 1417 – 1423.
- [13] Suciú and L. Morino "Nonlinear Steady Incompressible Lifting – Surface Analysis with Wake Roll-Up", AIAA Journal, Vol. 15, NO. 1, January 1977.

بحث توزيع الحمل والضغط على الجناح مع التفاف دوامات الأثر لطائرة ذات سرعة واطئة

ليث وضاح اسماعيل

قسم هندسة المواد / الجامعة التكنولوجية

الخلاصة

يتضمن البحث الحالي طريقة تحليل أولية يمكن استخدامها لحساب توزيع الاحمال والضغط على الاجنحة في السرع الواطئة مع وجود ظاهرتي انفصال الجريان والتفاف دوامات الأثر. حيث تم ربط طريقة اشربة الدوامات مع نظرية الخط الحامل العددية بواسطة اسلوب تكراري متضمناً نموذج انفصال الجريان ونموذج التفاف دوامات الاثر. تم بناء عدة برامج في الحاسوب باستخدام لغة فورتران وتمتاز هذه البرامج بكفائتها واستقراريتها.

تم بحث امكانية الطريقة الحالية من خلال عدد مختلف من الحالات لأجنحة ذات مقاطع مختلفة (NACA 0012 and GA(W)-1) لنسب باعية وزوايا هجوم مختلفة، تضمنت النتائج منحنيات الرفع والكبح وتوزيع الرفع والضغط على طول باع الجناح، تم الاخذ بنظر الاعتبار تأثير زوايا الهجوم والنسب الباعية على التفاف دوامات الاثر. توزيع الضغط على الاجنحة بين ان هناك منطقة الضغط الثابت على السطح العلوي للأجنحة قرب الحافة الخلفية في منتصف الجناح، كما وجد ان هناك منطقة انفصال للجريان على السطح العلوي للأجنحة. قورنت النتائج المستحصلة مع أخرى تم الحصول عليها من بحوث منشورة وقد ظهر تقارب جيد بينها.

النتائج المستحصلة بينت ان الطريقة الحالية قد تمكنت من الاحاطة بمختلف ظواهر الجريان على الاجنحة مثل انفصال الجريان والتفاف دوامات الاثر.